Food Chemistry: X 24 (2024) 102008

Contents lists available at ScienceDirect

Food Chemistry: X

journal homepage: www.sciencedirect.com/journal/food-chemistry-x

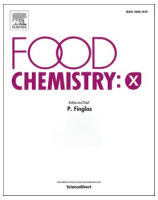

Comparative analysis of key aroma compounds in air-frying roasted pork from five species

Lin Li [a], Pingping Huang [b], Rujie Yang [b], Jingyu Li [b], Yuping Zhang [b], Junke Li [b], Jianjun Li [c], Jianmei Zhang [c], Nigel P. Brunton [d], Huan Liu [b,*], Xiangru Wei [d,*]

[a] Yantai Food and Drug Inspection and Testing Center, Yantai 264035, Shandong, China
[b] School of Food Engineering, Yantai Key Laboratory of Nanoscience and Technology for Prepared Food, Yantai Engineering Research Center of Green Food Processing and Quality Control, Bionanotechnology Institute, Ludong University, Yantai 264025, China
[c] Yantai Xiwang Foods Co., Ltd., Yantai 264025, China
[d] School of Agriculture and Food Science, University College Dublin, Dublin 4, Ireland

ARTICLE INFO

Keywords:
Roasted pork
Aroma profile
GC-O-MS
Biomarker
Sensory evaluation

ABSTRACT

The popularity of roasted pork among Chinese consumers is largely attributed to its rich aroma profile. However, the suitability of different pork species for roasting remains uncertain. In this study, the effect of various pork species on the aroma profiles of roasted pork was systematically investigated using gas chromatography-olfactometry-mass spectrometry (GC-O-MS). The results indicated that the roasted pork from five different species exhibited rich roasty, meaty, and fatty notes. Fifty-two aroma compounds were identified, with seven key odorants, including pyrazines and aldehydes, being recognized as primary contributors to the aroma. The orthogonal partial least squares discriminant analysis (OPLS-DA) effectively distinguished the aroma profiles of the five pork species. Twelve aroma compounds displayed variable importance in projection (VIP) scores exceeding 1, with butyrolactone being identified as a potential biomarker. Among the species, Tibetan and Min pigs were found to be the most suitable for roasting, with Min pigs showing particular promise.

1. Introduction

China possesses the most diverse pig species resources globally. In 2023, pork production in China reached 57.94 million tons, representing a 4.6 % increase compared to 2022. Over 60 pig breeds have been identified in China, including 48 local breeds and 12 cultivated ones. The roasted pork is widely favored in China due to its appealing aromas. A previous study identified over 40 odorants in Mini-pig roasted pork using simultaneous distillation-solvent extraction (SDE) and gas chromatography-olfactometry (GC-O), including roasty 2,5-dimethylpyrazine, meaty 2-acetylthiazole, fatty (E)-2-nonenal, and grassy hexanal (Xie, Sun, Zheng, & Wang, 2008). The synergy of fatty acids, free radicals, secondary oxidation products, and spices leads to an increase in both the concentration and diversity of aroma compounds during pan-heating, generating distinct aroma profiles, such as aldehydes (Wang et al., 2023). Our recent study revealed that air-frying, microwave heating, superheated steam, and traditional charcoal roasting all produce strong aroma profiles in roasted pork, with air-frying emerging as an effective alternative to traditional charcoal roasting technology due to its efficient heating and production of richer aroma compounds (Liu et al., 2024). Further investigation based on air-frying technology demonstrats that neutral lipids and phospholipids, including triglycerides, phosphatidylcholine, phosphatidylethanolamine, and phosphatidylserine, significantly contribute to the formation and retention of key aroma compounds, such as hexanal and 3,5-dimethyl-2-ethylpyrazine, in air-frying roasted pork (Liu et al., 2023). These findings suggest that both endogenous and exogenous factors, including chemical compositions, roasting methods, and roasting time, influence the production of aroma compounds in roasted pork. The species is a key factor affecting aroma variability in meat, ultimately determining the sensory attributes of the final product (Fan et al., 2018). Despite this, a comprehensive understanding of how different species affect aroma compound variations in roasted pork and their association with sensory evaluations remains elusive.

Yan et al. develope a metabolic approach using supervised OPLS-DA to identify biomarkers for differentiating roasted pork at various heating times, identifying five biomarkers, including creatine and creatinine (Yan et al., 2021). Mu et al. apply GC–MS and OPLS-DA to differentiate

* Corresponding author.
E-mail addresses: sd_lh1990@126.com (H. Liu), xiangru.wei@ucdconnect.ie (X. Wei).

https://doi.org/10.1016/j.fochx.2024.102008
Received 4 October 2024; Received in revised form 3 November 2024; Accepted 13 November 2024
Available online 15 November 2024

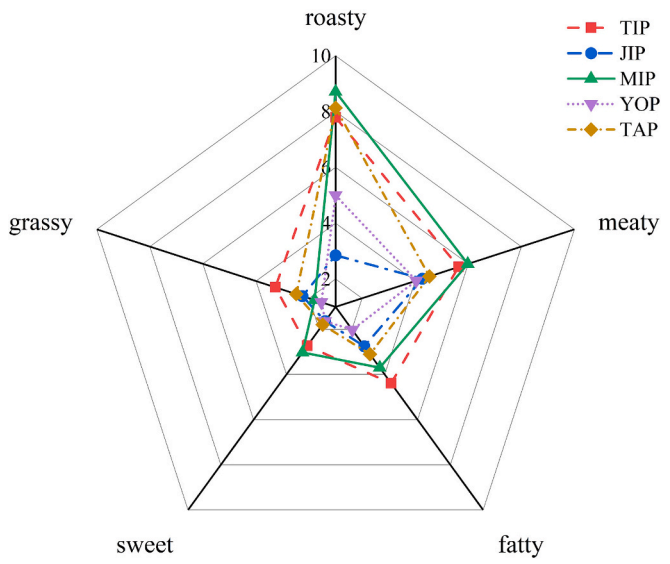

Fig. 1. Sensory evaluation of aroma profiles in roasted pork from five species.

raw and roasted beef with varying fat content, identifying benzaldehyde, 2,3-pentanedione, and 2-butanone as key contributors to aroma differences based on fat concentration (Mu, Ni, Zhu, Boesveldt, & Stieger, 2023). Our previous study identifies furaldehyde, 2,4-decadienal, and 1-hexanol as potential biomarkers for distinguishing roasted pork, beef, lamb, chicken, duck, and goose using GC–MS and PLS-DA (Shi et al., 2024). The multivariate statistical analysis combined with volatile compound profiling has also proven effective in characterizing Tibetan pork from four provinces (Zhao et al., 2023). Recently, our group further identifies acetic acid methyl ester as a key biomarker in differentiating roasted mutton using GC-O-MS, lipidomics, and OPLS-DA (Liang et al., 2024). Therefore, GC-O-MS combined with OPLS-DA offers a reliable method for identifying biomarkers that differentiate roasted pork from various species.

The choice of extraction methods significantly affects the identification and quantification of aroma compounds in food products (Majcher & Jeleń, 2009; Murat, Gourrat, Jerosch, & Cayot, 2012; Nie et al., 2024). The solid-phase microextraction (SPME) offers advantages such as rapid extraction and broad application, but its limitations in accurate quantification restrict its use (Murat et al., 2012). The SPME combined with semi-quantitative internal standard methods is widely applied to explore aroma compound diversity (Edgar Herkenhoff, Brödel, & Frohme, 2024). The solvent-assisted flavor evaporation (SAFE) coupled with GC-O-MS is often employed for detailed elucidation of molecular structures and accurate concentrations of key odorants (Dach & Schieberle, 2021). For example, Gerlach et al. apply SAFE-GC-O-MS to identify 16, 12, and 14 key aroma compounds in the fat of boar, female pigs, and castrated male pigs, respectively (Gerlach et al., 2018). Additionally, fifteen compounds were identified as key contributors to the aroma profile of dry-rendered beef fat, including (*E, E*)-2,4-nonadienal (Yang, Pei, Du, & Xie, 2023). Therefore, SAFE-GC-O-MS is a necessary approach to elucidate key odorants in roasted pork from different species.

To date, there has been no systematic study on the aroma differences and roasting suitability of pork from various species. This study aims to (i) investigate the aroma profile differences in roasted pork from five species based on sensory evaluation, (ii) identify the molecular structures of key odorants using SAFE-GC-O-MS and four identification methods, (iii) elucidate the contribution of key aroma compounds to the overall aroma profiles using odor activity values (OAVs) and GC-O, and (iv) identify biomarkers for distinguishing roasted pork from the five species using OPLS-DA. The findings from this study will aid in linking sensory evaluations with aroma compounds, providing insights into the aroma variability of different meat products and their underlying causes. Additionally, the study will offer theoretical support for selecting optimal pig species for roasted pork and guiding new product development.

Table 1
Identification of aroma compounds in roasted pork from five species.

Compounds [a]	RI [b]		Identification [e]	compounds	RI		identification
	Literature [c]	Calculation [d]			literature	calculation	
acetic acid methyl ester	864	864	MS, RI	2-ethyl-1-hexanol	1470	1472	MS, RI
propanoic acid ethyl ester	949	948	MS, RI, O, S	pyrrole	1490	1487	MS, RI
2-methyl-3-buten-2-ol	1036	1029	MS, RI	benzaldehyde	1495	1489	MS, RI, O, S
2-methyl-2-butenal	1076	1073	MS, RI	5-methyl-2,3-diethylpyrazine	1497	1490	MS, RI, O, S
hexanal	1078	1078	MS, RI, O, S	propanoic acid	1520	1511	MS, RI
1-butanol	1134	1131	MS, RI	2-methylpropanoic acid	1544	1543	MS, RI
pyridine	1170	1172	MS, RI	butyrolactone	1595	1590	MS, RI
2,3-dihydro-4-methylfuran	1170	1176	MS, RI	butanoic acid	1607	1601	MS, RI, O, S
dihydro-2-methyl-3(2*H*)-furanone	1242	1241	MS, RI	benzeneacetaldehyde	1619	1616	MS, RI, O, S
methylpyrazine	1247	1244	MS, RI, O, S	2-furanmethanol	1635	1636	MS, RI
1-hydroxy-2-propanone	1275	1274	MS, RI	1-methyl-2-pyrrolidinone	1652	1649	MS, RI
4-methyl-2-pentanol	1281	1288	MS, RI	2-acetyl-3-methylpyrazine	1640	1662	MS, RI, O, S
prenol	1301	1303	MS, RI	(*E*)-2-methyl-5-(1-propenyl)pyrazine	1635	1686	MS, RI
2,5-dimethylpyrazine	1308	1305	MS, RI, O, S	pentanoic acid	1713	1712	MS, RI
ethylpyrazine	1311	1310	MS, RI	2(5*H*)-furanone	1716	1717	MS, RI
2,3-dimethylpyrazine	1326	1322	MS, RI	hexanoic acid	1810	1817	MS, RI
2-ethyl-6-methylpyrazine	1363	1362	MS, RI, O, S	benzyl alcohol	1844	1848	MS, RI
2-ethyl-5-methylpyrazine	1376	1368	MS, RI, O, S	heptanoic acid	1923	1923	MS, RI
nonanal	1374	1378	MS, RI, O, S	1-(1H-pyrrol-2-yl) ethanone	1949	1941	MS, RI
trimethylpyrazine	1381	1381	MS, RI, O, S	phenol	1978	1976	MS, RI
5-ethyl-2,3-dimethylpyrazine	1416	1421	MS, RI, O, S	pantolactone	1998	2000	MS, RI
acetic acid	1429	1427	MS, RI	2-pyrrolidinone	2017	2013	MS, RI
1-octen-3-ol	1430	1432	MS, RI, O, S	octanoic acid	2030	2029	MS, RI
2-ethyl-3,5-dimethylpyrazine	1440	1438	MS, RI, O, S	p-cresol	2059	2054	MS, RI
methional	1450	1441	MS, RI, O, S	nonanoic acid	2124	2119	MS, RI
tetramethylpyrazine	1457	1452	MS, RI	dimethyl phthalate	2276	2277	MS, RI

[a] Aroma compounds in roasted pork from five species. [b] Retention index. [c] reported data. [d] calculated data based on n-alkanes. [e] MS, mass spectrum; RI, retention index; O, odor qualities; S, authentic flavor standards.

Table 2
Standard calibration curves of aroma compounds (OAVs >1) in roasted pork from five species.

Compounds	Ion fragments [a]	Standard calibration curves [b]	R^2
propanoic acid ethyl ester	43, 61, 70	y = 2.4651× + 0.0071	0.9997
hexanal	41, 44, 56	y = 2.0777× + 0.1966	0.9982
2-methylpyrazine	40, 67, 94	y = 0.8484× + 0.0066	0.9995
2,5-dimethylpyrazine	39, 42, 108	y = 0.8073× + 0.0003	0.9982
2-ethyl-6-methylpyrazine	94, 121, 122	y = 0.2944× + 0.0068	0.9995
2-ethyl-5-methylpyrazine	44, 121, 122	y = 1.6787×-0.0041	0.9985
nonanal	41, 44, 57	y = 1.2579× + 0.0108	0.9987
trimethylpyrazine	42, 81, 122	y = 0.7356× + 0.0101	0.9997
5-ethyl-2,3-dimethylpyrazine	42, 135, 136	y = 1.3972× + 0.0047	0.9991
1-octen-3-ol	41, 43, 57	y = 0.5068× + 0.0270	0.9986
2-ethyl-3,5-dimethylpyrazine	42, 135, 136	y = 0.4020× + 0.0044	0.9996
methional	47, 48, 104	y = 2.5707× + 0.0054	0.9996
benzaldehyde	77, 105, 106	y = 0.9524× + 0.0009	0.9998
5-methyl-2,3-diethylpyrazine	135, 149, 150	y = 1.2711× + 0.0009	0.9989
butanoic acid	43, 60, 73	y = 0.7830× + 0.0567	0.9961
benzeneacetaldehyde	65, 91, 92	y = 0.6076× + 0.0095	0.9995
2-acetyl-3-methylpyrazine	42, 43, 136	y = 2.3980×-0.0025	0.9982

[a] Selected ion fragments on the basis of the authentic flavor standards. [b] Equations of standard calibration curves, where x is the peak area ratio of flavor standards to internal standard and y is their concentration ratio.

2. Materials and methods

2.1. Sample collection and grouping

A total of fifteen pigs were selected from the farms in 2024, including five species: Tibetan pigs (TIP), Jinhua pigs (JIP), Min pigs (MIP), Yorkshire pigs (YOP), and Taihu pigs (TAP), with three pigs from each species. The pigs were slaughtered following the guidelines of the Animal Care and Use Committee of Ludong University (LDU-IRB202402006). Meanwhile, all pigs were slaughtered in commercial abattoirs following the international standard (ISO/TS 34700:2016). Briefly, the pigs were stunned using a captive bolt, followed by severing of the jugular veins and carotid arteries to induce the exsanguination, causing rapid heart failure and death. The pork muscle was frozen at −35 °C and transported to our laboratory using standard cold-chain logistics. The samples were then thawed in an incubator (MIR-154-PC, Panasonic, Japan) at 4 °C until reaching a core temperature of −4 °C. The samples were roasted within one week to minimize alterations in raw sample quality. For experimental purposes, the left tenderloin was used, and the muscle samples were cut into dimensions of 3 × 1.5 × 1.5 cm^3. The pork samples were roasted in a CKY-298 oven (German Pool (Hong Kong) Co., Ltd., Hongkong, China) at 230 °C for 15 min, achieving a core temperature of 74–78 °C. These roasting conditions were selected to attain optimal sensory qualities for the desired palatability.

The following aroma standards were purchased from Sigma-Aldrich (Shanghai, China): hexanal (98 %), nonanal (98 %), benzaldehyde (99.5 %), benzeneacetaldehyde (95 %), 1-octen-3-ol (98 %), butanoic acid (99 %), methylpyrazine (99 %), 2,5-dimethylpyrazine (98 %), trimethylpyrazine (99 %), 2-acetyl-3-methylpyrazine (98 %), methional (97 %), and propanoic acid ethyl ester (99 %). Additionally, 5-ethyl-2,3-dimethylpyrazine (98 %), 2-ethyl-3,5-dimethylpyrazine (98 %), 5-methyl-2,3-diethylpyrazine (98 %), 2-ethyl-6-methylpyrazine (98 %), and 2-ethyl-5-methylpyrazine (98 %) were procured from Aladdin (Beijing, China). 2-methyl-3-heptanone (99 %) and n-alkanes (C_7-C_{40}, 97 %) were sourced from Dr. Ehrenstorfer and O2si Smart Solutions.

2.2. Sensory evaluation

Prior informed consent for sensory evaluation was obtained from all participants. The experiment adhered to protocols approved by the Human Research Ethics Committee of Ludong University (LDU-IRB202405001), ensuring the protection of participants' rights and privacy. Twenty-five trained panelists aged from 24 to 35 (fourteen females, eleven males) participated in the sensory evaluation, following the guidelines of ISO 4121:2003. The panelists evaluated the roasted pork samples based on five sensory attributes: roasty, meaty, fatty, grassy, and sweet notes. Each sample was coded with a random 3-digit number and evaluated at 25 °C. A 10-point scale (0 = absent, 10 = strong) was used for rating each attribute (Phetsang et al., 2021).

2.3. SAFE-GC-O-MS analysis

The minced pork (50 g) was combined with 25 μL of 2-methyl-3-heptanone (2 μg/μL) and extracted with 50 mL of dichloromethane at 42 °C for 3 h according to our previous study (Liu et al., 2023). After the extraction for three times, the extracts were pooled. The SAFE technology was immediately employed to isolate volatile organic compounds. The distillate was concentrated to 2 mL using a Vigreux column (50 × 1 cm inner diameter) and further reduced to 200 μL under a nitrogen stream.

Aroma compounds were analyzed using a Thermo Scientific™ TRACE™ 1310 gas chromatograph coupled with a TSQ 9000 mass spectrometer (Thermo Scientific, Bremen, Germany) and olfactory detection port (OP275 Pro II, GL Sciences Inc., Japan). A polar DB-Wax column (30 m × 0.25 mm × 0.25 μm) was applied to extract odorants. The helium (purity: 99.99 %) was used as the carrier gas. The temperatures for MS transfer line and ion source were set to 240 °C and 260 °C, respectively. The electron impact (EI) mass spectrometry was conducted at an ionization energy of 70 eV with a scanning range of 40 to 500 *m/z*. Analytical conditions followed those described in our previous study (Liu, Li, et al., 2023).

2.4. Identification and quantification analysis

Aroma compounds in roasted pork from the five species were identified using four methods: mass spectral library (NIST 2020), retention index, odor quality, and comparison with authentic standards. RIs were determined using n-alkanes (C_7-C_{40}) as reference compounds. Peak times of the authentic standards were compared to the sample peaks under identical analytical conditions.

The aroma compounds were quantified (semi-quantitative analysis) by dividing the peak areas of the compounds of interest by the peak area of 2-methyl-3-heptanone as internal standard (Selli, Gubbuk, Kafkas, & Gunes, 2012). The aroma compounds with OAVs >1 were quantified using the standard curve method in selected ion monitoring (SIM) mode, as described in a prior study (Liu, Li, et al., 2023). Briefly, the mixed authentic flavor standards with gradient concentrations and 2-methyl-3-heptanone (1000 ng/g) were placed into the dichloromethane. The calibration equations were established based on the concentration ratios and their ion peak area ratios.

2.5. Determination of key aroma compounds

The OAVs were calculated by dividing the concentration of an aroma compound by its medium odor threshold (Schieberle, 1995). The aroma compounds with OAVs >1 were considered significant contributors to the overall aroma profile of roasted pork. Compounds with OAVs <1 were considered to have minimal contributions.

2.6. Statistical analysis

Data were presented as means ± standard deviations. The statistical

Table 3
Concentrations of aroma compounds in roasted pork from five species.

Compounds (ng/g)	TIP	JIP	MIP	YOP	TAP
acetic acid methyl ester	420.86 ± 9.75^{a}	309.75 ± 7.89^{c}	403.97 ± 7.57^{a}	325.11 ± 6.49^{c}	350.94 ± 2.79^{b}
propanoic acid ethyl ester	101.61 ± 15.06^{b}	91.22 ± 2.50^{b}	102.18 ± 7.92^{b}	136.88 ± 11.31^{a}	76.06 ± 3.39^{b}
2-methyl-3-buten-2-ol	258.13 ± 2.71^{b}	260.66 ± 9.38^{b}	253.66 ± 7.35^{b}	291.80 ± 3.26^{a}	274.81 ± 17.78^{ab}
2-methyl-2-butenal	45.83 ± 1.34b^{c}	50.52 ± 2.69^{ab}	40.78 ± 2.40^{c}	46.74 ± 1.44^{bc}	55.47 ± 4.41^{a}
hexanal	1159.90 ± 33.72^{a}	472.74 ± 6.16^{b}	281.32 ± 4.98^{c}	293.71 ± 2.99^{c}	311.85 ± 9.15^{c}
1-butanol	0^{b}	0^{b}	0^{b}	0^{b}	50.22 ± 1.44^{a}
3-penten-2-ol	14,016.10 ± 95.21^{b}	14,903.80 ± 144.35^{b}	12,898.49 ± 318.49^{c}	14,580.75 ± 227.11^{b}	17,864.52 ± 631.46^{a}
2-propenoic acid butyl ester	0^{b}	0^{b}	0^{b}	0^{b}	301.26 ± 19.55^{a}
pyridine	57.86 ± 0.22^{b}	0^{c}	49.96 ± 1.82^{b}	47.47 ± 2.95^{b}	161.92 ± 7.32^{a}
2,3-dihydro-4-methylfuran	27.50 ± 0.23^{b}	33.80 ± 1.27^{a}	28.69 ± 1.02^{b}	0^{c}	35.92 ± 1.58^{a}
dihydro-2-methyl-3(2H)-furanone	45.10 ± 7.04^{ab}	0^{c}	55.54 ± 2.03^{a}	42.27 ± 1.89^{b}	51.33 ± 2.84^{ab}
methylpyrazine	136.81 ± 3.92^{b}	92.28 ± 1.60^{d}	294.59 ± 9.85^{a}	113.11 ± 3.05^{c}	101.29 ± 4.61^{cd}
1-hydroxy-2-propanone	3098.44 ± 20.36^{c}	2777.41 ± 72.98^{cd}	4473.07 ± 182.25^{a}	4009.36 ± 94.53^{b}	2633.71 ± 112.08^{d}
4-methyl-2-pentanol	8265.92 ± 63.90^{cd}	8936.48 ± 171.42^{bc}	7784.98 ± 225.54^{d}	9290.93 ± 235.47^{b}	10,996.42 ± 507.37^{a}
prenol	118.89 ± 0.10^{a}	100.12 ± 6.80^{ab}	93.58 ± 4.99^{b}	110.36 ± 3.18^{a}	108.53 ± 5.91^{ab}
2,5-dimethylpyrazine	147.60 ± 4.23^{b}	98.82 ± 1.77^{d}	379.82 ± 13.75^{a}	124.16 ± 3.79^{c}	71.88 ± 4.61^{e}
ethylpyrazine	25.34 ± 0.49^{b}	19.13 ± 1.01^{c}	40.04 ± 1.64^{a}	20.24 ± 0.38^{c}	13.02 ± 0.60^{d}
2,3-dimethylpyrazine	52.99 ± 0.57^{b}	23.43 ± 0.56^{d}	89.93 ± 3.86^{a}	34.66 ± 4.03^{c}	39.79 ± 2.40^{c}
2-ethyl-6-methylpyrazine	44.26 ± 0.84^{b}	19.00 ± 0.18^{d}	63.71 ± 2.00^{a}	27.19 ± 0.69^{c}	26.18 ± 1.32^{c}
2-ethyl-5-methylpyrazine	150.69 ± 4.40^{b}	79.90 ± 1.20^{c}	258.31 ± 9.73^{a}	74.12 ± 2.34^{c}	63.38 ± 4.93^{c}
nonanal	109.10 ± 3.20^{a}	66.26 ± 1.37^{c}	62.48 ± 1.90^{c}	60.77 ± 1.07^{c}	86.61 ± 6.95^{b}
trimethylpyrazine	329.54 ± 9.38^{b}	159.26 ± 3.02^{d}	524.18 ± 17.54^{a}	228.48 ± 6.38^{c}	205.32 ± 12.30^{c}
5-ethyl-2,3-dimethylpyrazine	254.90 ± 8.04^{b}	81.04 ± 1.32^{d}	331.41 ± 11.11^{a}	109.29 ± 3.03^{c}	122.54 ± 8.94^{c}
acetic acid	365.60 ± 24.42^{d}	701.06 ± 32.82^{b}	1079.39 ± 15.63^{a}	463.03 ± 10.96^{c}	344.08 ± 21.66^{d}
1-octen-3-ol	75.56 ± 1.45^{a}	39.96 ± 0.82^{d}	58.38 ± 0.80^{b}	51.41 ± 1.06^{c}	50.10 ± 1.74^{c}
2-furaldehyde	9.64 ± 0.13^{b}	12.23 ± 2.06^{b}	17.19 ± 0.51^{a}	0^{c}	0^{c}
2-ethyl-3,5-dimethylpyrazine	31.49 ± 0.95^{b}	15.78 ± 0.18^{d}	44.06 ± 1.26^{a}	18.04 ± 0.43^{cd}	19.61 ± 1.02^{c}
methional	155.22 ± 4.94^{c}	173.45 ± 7.76^{bc}	211.71 ± 8.66^{a}	106.20 ± 10.85^{cd}	99.84 ± 4.49^{d}
tetramethylpyrazine	13.34 ± 0.39^{c}	0^{e}	15.81 ± 0.76^{b}	10.41 ± 0.34^{d}	20.36 ± 1.44^{a}
2-ethyl-1-hexanol	33.26 ± 0.08^{b}	26.10 ± 0.01^{c}	15.02 ± 1.02^{d}	35.06 ± 0.43^{ab}	37.00 ± 2.29^{a}
pyrrole	51.47 ± 0.22^{a}	41.42 ± 1.31^{b}	0^{c}	0^{c}	40.87 ± 2.02^{b}
benzaldehyde	281.13 ± 6.62^{b}	196.07 ± 3.60^{d}	321.46 ± 11.28^{a}	251.09 ± 7.18^{c}	227.66 ± 14.46^{c}
5-methyl-2,3-diethylpyrazine	19.65 ± 0.58^{b}	0^{d}	23.31 ± 0.45^{a}	11.62 ± 0.45^{c}	20.86 ± 1.45^{b}
propanoic acid	26.13 ± 0.45^{b}	19.20 ± 0.57^{c}	44.55 ± 1.36^{a}	21.46 ± 0.63^{c}	12.32 ± 1.49^{d}
2-methylpropanoic acid	22.27 ± 0.22^{a}	0^{b}	0^{b}	24.46 ± 1.88^{a}	0^{b}
butyrolactone	513.13 ± 4.72^{a}	114.02 ± 2.25^{e}	340.63 ± 11.75^{c}	172.56 ± 5.36^{d}	448.01 ± 24.18^{b}
butanoic acid	559.69 ± 12.04^{d}	1575.13 ± 36.66^{a}	781.19 ± 24.11^{c}	1004.18 ± 24.51^{b}	480.59 ± 27.07^{d}
benzeneacetaldehyde	370.13 ± 12.36^{a}	158.52 ± 2.42^{d}	334.67 ± 6.13^{b}	177.01 ± 5.76^{d}	207.55 ± 13.97^{c}
2-furanmethanol	74.43 ± 0.79^{b}	14.90 ± 0.92^{e}	95.37 ± 2.36^{a}	24.12 ± 0.88^{d}	43.96 ± 2.63^{c}
1-methyl-2-pyrrolidinone	10.77 ± 0.64^{d}	12.73 ± 0.37^{cd}	27.68 ± 0.61^{b}	20.23 ± 2.44^{bc}	87.90 ± 5.79^{a}
2-acetyl-3-methylpyrazine	19.25 ± 0.73^{a}	6.87 ± 1.06^{b}	0^{c}	17.98 ± 0.71^{a}	7.56 ± 0.75^{b}
(*E*)-2-methyl-5-(1-propenyl)pyrazine	37.76 ± 0.25^{b}	12.01 ± 0.25^{d}	60.28 ± 1.01^{a}	12.87 ± 0.47^{d}	19.16 ± 1.44^{c}
pentanoic acid	42.19 ± 0.17^{b}	37.09 ± 4.85^{b}	65.56 ± 1.72^{a}	61.29 ± 1.78^{a}	0^{c}
2(5H)-furanone	283.09 ± 2.18^{b}	0^{c}	375.81 ± 11.88^{a}	0^{c}	0^{c}
hexanoic acid	228.05 ± 2.00^{cd}	507.63 ± 12.21^{a}	142.06 ± 57.21^{d}	369.86 ± 13.24^{b}	232.36 ± 19.14^{c}
benzyl alcohol	10.87 ± 0.41^{b}	10.29 ± 0.64^{b}	0^{c}	16.53 ± 2.22^{a}	12.42 ± 0.67^{b}
heptanoic acid	18.47 ± 0.59^{c}	0^{d}	34.17 ± 0.68^{a}	34.42 ± 2.91^{a}	23.98 ± 1.07^{b}
1-(1H-pyrrol-2-yl) ethanone	175.71 ± 2.72^{c}	362.83 ± 4.88^{b}	653.5 ± 19.22^{a}	164.55 ± 16.52^{c}	71.14 ± 4.45^{d}
phenol	18.00 ± 0.91^{cd}	15.55 ± 0.63^{d}	28.43 ± 0.85^{a}	19.78 ± 0.50^{c}	23.12 ± 1.28^{b}
pantolactone	218.43 ± 6.60^{c}	15.55 ± 0.63^{d}	367.97 ± 9.74^{b}	358.31 ± 5.65^{b}	799.82 ± 51.59^{a}
2-pyrrolidinone	129.69 ± 4.33^{b}	0^{c}	0^{c}	0^{c}	220.52 ± 13.51^{a}
octanoic acid	32.07 ± 2.15^{d}	96.63 ± 3.01^{a}	49.27 ± 1.31^{c}	72.42 ± 3.31^{b}	78.60 ± 10.09^{b}
p-cresol	0^{d}	22.37 ± 0.47^{b}	0^{d}	18.28 ± 0.55^{c}	28.00 ± 1.44^{a}
nonanoic acid	0^{d}	22.31 ± 0.85^{a}	11.31 ± 0.14^{c}	0^{d}	23.03 ± 2.46^{a}
dimethyl phthalate	95.61 ± 4.79^{d}	168.92 ± 3.38^{c}	295.32 ± 9.16^{ab}	316.93 ± 9.99^{a}	269.06 ± 18.35^{b}
tetradecanoic acid	0^{b}	0^{b}	0^{b}	0^{b}	35.37 ± 0.71^{a}

The different superscript letters (a, b, c, d, e) in the same row indicated significant differences ($p < 0.05$).

significance ($p < 0.05$) among different roasted pork samples was assessed using Fisher's protected least significant difference (LSD) test. The Origin 2024 (OriginLab Corporation, USA) and SIMCA 14.1 (Umetrics Co., Ltd., Sweden) were used for graphing. The discrimination between samples was conducted using OPLS-DA. The biomarkers were identified based on variable importance in projection (VIP) scores >1 and $p < 0.05$.

3. Results and discussion

3.1. Identification and quantitation of aroma compounds in roasted pork

As shown in Fig. 1, the roasted pork from the five species exhibited distinct roasty, meaty, fatty, sweet, and grassy notes. Overall, the MIP sample was rated higher for roasty, meaty, and sweet aromas compared to TIP, JIP, YOP, and TAP samples. Meanwhile, the TIP sample showed the highest intensities for fatty and grassy notes among all samples. Conversely, the JIP sample exhibited the weakest aroma profile, followed by the YOP sample. On the other hand, the roasted pork from four species (TIP, MIP, YOP, TAP) all demonstrated the strongest roasty notes, followed by meaty and fatty notes. The sweet and grassy notes were generally weaker across all samples compared to other aroma descriptors. This result is in accordance with the findings of Gąsior et al. (2021), where the roasted white Kołuda goose exhibites high intensities for roasty, meaty, and fatty notes, alongside lower sweet and grassy notes. The aroma profile of roasted pork results from a combination of individual aroma compounds and their interactive effects among which a hypo-addition partial addition effect was observed between 1-octen-3-

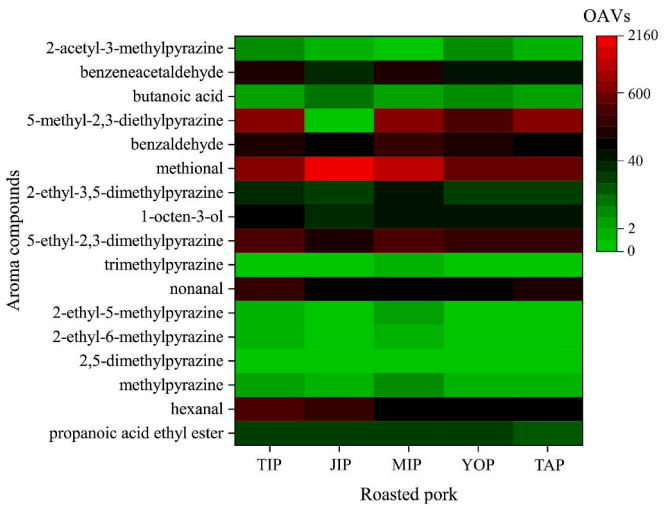

Fig. 2. OAVs of aroma compounds (OAVs >1) in roasted pork from five species.
The color intensity ranged from green to red represented the increased concentration. (For interpretation of the references to color in this figure legend, the reader is referred to the web version of this article.)

ol and certain acids (Niu, Zhang, Xiao, & Zhu, 2020).

As summarized in Table 1, fifty-two odorants were identified in roasted pork from the five species using mass spectrum search, retention index calculation, odor quality evaluation, and authentic flavor standards comparison. A total of 47, 41, 43, 43, and 48 odorants were detected in TIP, JIP, MIP, YOP, and TAP samples, respectively (Table 3). These aroma compounds included aldehydes, ketones, acids, esters, alcohols, phenols, nitrogen-containing compounds, and sulfur-containing compounds. Notably, thirty-three aroma compounds were detected in all roasted pork samples. Among these, thirteen pyrazines, including 2,5-dimethylpyrazine, trimethylpyrazine, and 5-ethyl-2,3-dimethylpyrazine, were identified, representing the highest proportion of the aroma compounds. This contrasts with a previous study where alcohols were the predominant aroma compounds in smoked duck during storage (Jo, An, Arshad, & Kwona, 2018). These results suggest that pyrazines contribute significantly to the roasty aroma of roasted pork due to their molecular properties (Zhu et al., 2021). The characteristic ion fragments (m/z) of the aroma compounds with OAVs >1 were used to establish calibration curves (Table 2). The high correlation coefficients (R^2 > 0.99) for all odorants indicated excellent linearity. The concentrations of all odorants in roasted pork from the five species are presented in Table 3. Among these, 3-penten-2-ol (12,898.49–17,864.52 ng/g) and 4-methyl-2-pentanol (7784.98–10,996.42 ng/g) were the most abundant compounds. Other major aroma compounds with high concentrations included 1-hydroxy-2-propanone (2633.71–4473.07 ng/g), butanoic acid (480.59–1575.13 ng/g), acetic acid (344.08–1079.39 ng/g), butyrolactone (114.02–513.13 ng/g), and hexanoic acid (142.06–507.63 ng/g). This phenomenon is in accordance with the study, among which the butyrolactone and hexanoic acid are also detected in the braised pork (Yao et al., 2024). Several aroma compounds, including 2,3-dihydro-4-methylfuran, ethylpyrazine, 2-furaldehyde, 2-ethyl-3,5-dimethylpyrazine, tetramethylpyrazine, 2-ethyl-1-hexanol, 5-methyl-2,3-diethylpyrazine, propanoic acid, 2-methylpropanoic acid, 2-acetyl-3-methylpyrazine, benzyl alcohol, heptanoic acid, phenol, p-cresol, nonanoic acid, and tetradecanoic acid, were present at levels below 50 ng/g. The 2-furaldehyde is detected in roasted Mini-pig pork, with a relatively low concentration ranging between 0.05 % and 0.10 % (Xie et al., 2008). Overall, 11 out of 13 pyrazines in the MIP sample exhibited the highest concentrations, followed by the TIP sample, with the exception of tetramethylpyrazine and 2-acetyl-3-methylpyrazine. This suggested that the MIP sample produced a more distinct roasty aroma compared to other roasted pork samples, consistent with the aroma profile results, where MIP and TIP samples had significantly higher roasty intensities than JIP, YOP, and TAP samples. This observation aligns with previous findings, where roasted barley and rye brews with higher concentrations of pyrazines, such as 2-ethyl-3,5-dimethylpyrazine, emerge stronger roasty intensities compared to roasted chicory and sugar beet brews with lower pyrazine concentrations (Majcher, Klensporf-Pawlik, Dziadas, & Jeleń, 2013).

3.2. Determination of key aroma compounds in roasted pork

The contribution of each aroma compound to the overall aroma of a product depends not only on its concentration but also on its OAV. As shown in Fig. 2, color coding was graded according to the scale from green to red with the relative intensity increasing from greener to redder box character. A total of 15, 12, 16, 13, and 13 aroma compounds with OAVs greater than 1 were identified in TIP, JIP, MIP, YOP, and TAP samples, respectively. The cumulative OAV of TIP (2611.32) was the highest, followed by JIP (2589.08) and MIP (2370.66). TAP (1686.62) and YOP (1379.13) showed the lowest OAVs. These findings suggested that TIP and JIP samples might have richer aroma profiles and stronger aroma intensities. Twelve odorants were common to all five roasted pork samples, including hexanal, nonanal, benzaldehyde, benzeneacetaldehyde, ethyl propanoate, 1-octen-3-ol, methylpyrazine, 5-ethyl-2,3-dimethylpyrazine, 2-ethyl-3,5-dimethylpyrazine, 5-methyl-2,3-diethylpyrazine, methional, and butanoic acid. The roasted pork from all species had high OAVs for methional (499.22–2154.14), 5-ethyl-2,3-dimethylpyrazine (81.04–331.44), hexanal (62.52–257.76), nonanal (60.77–109.10), benzaldehyde (65.36–93.71), and benzeneacetaldehyde (39.63–92.53). Moreover, the MIP had the highest cumulative OAV of pyrazines, which likely contributed to its more pronounced roasty aroma. The TIP contained compounds contributing to fatty and grassy aromas, such as nonanal, hexanal, ethyl propanoate, and 1-octen-3-ol. There was no significant difference in the cumulative OAVs of compounds with fatty and grassy notes across the other four roasted pork samples, ranging from 127.85 to 155.15. Additionally, the MIP (83.67) and TIP (92.53) had the highest OAVs for benzeneacetaldehyde, which contributed a sweet note. These results were consistent with the sensory evaluation, which indicated that MIP and TIP samples had the strongest aroma intensities, particularly for roasty, meaty, and sweet aromas.

The GC-O analysis reveals that 5-methyl-2,3-diethylpyrazine, 2-ethyl-5-methylpyrazine, and 2-methylpyrazine are key contributors to roasty aromas (Gąsior et al., 2021; Liu, Li, et al., 2023). Long-chain alkylated pyrazines may be formed through reactions between dihydropyrazines and aldehydes (Huang, Bruechert, Hartman, Rosen, & Ho, 1987). The synergistic reactions between Maillard reaction products and lipid oxidation products contribute to the formation of pyrazines, with the interaction of glycerine and triglycerides playing a role in the generation of methylpyrazines (Ho & Hartman, 1994). High-intensity ultrasound can promote aldol-type condensation between glucose and glycine, resulting in the formation of 2-methylpyrazine, 2,6-dimethylpyrazine, and 2-ethyl-5-methylpyrazine (Zhang et al., 2022). The methional is primarily produced through methionine degradation under the thermal treatment (Yu & Ho, 1995). Meanwhile, the phospholipids and triacylglycerols contribute to the formation of carbonyl-containing aroma compounds, such as hexanal (Dannenberger et al., 2006; Liang et al., 2024). The increased concentrations of aroma compounds, including aldehydes, ketones, and alcohols, may be due to the breakdown of polyunsaturated bonds in phosphatidylcholine, phosphatidylethanolamine, and triglycerides (Liu, Ma, et al., 2024). The retention of certain aroma compounds, such as 5-ethyl-2,3-dimethylpyrazine, hexanal, and nonanal, may be attributed to their interaction with triglycerides (TG), including TG (16:0_16:0_18:0) (Liu, Liu, et al., 2023). Proteins like actomyosin and G-actin are also involved in binding carbonyl-containing aroma compounds, depending on protein

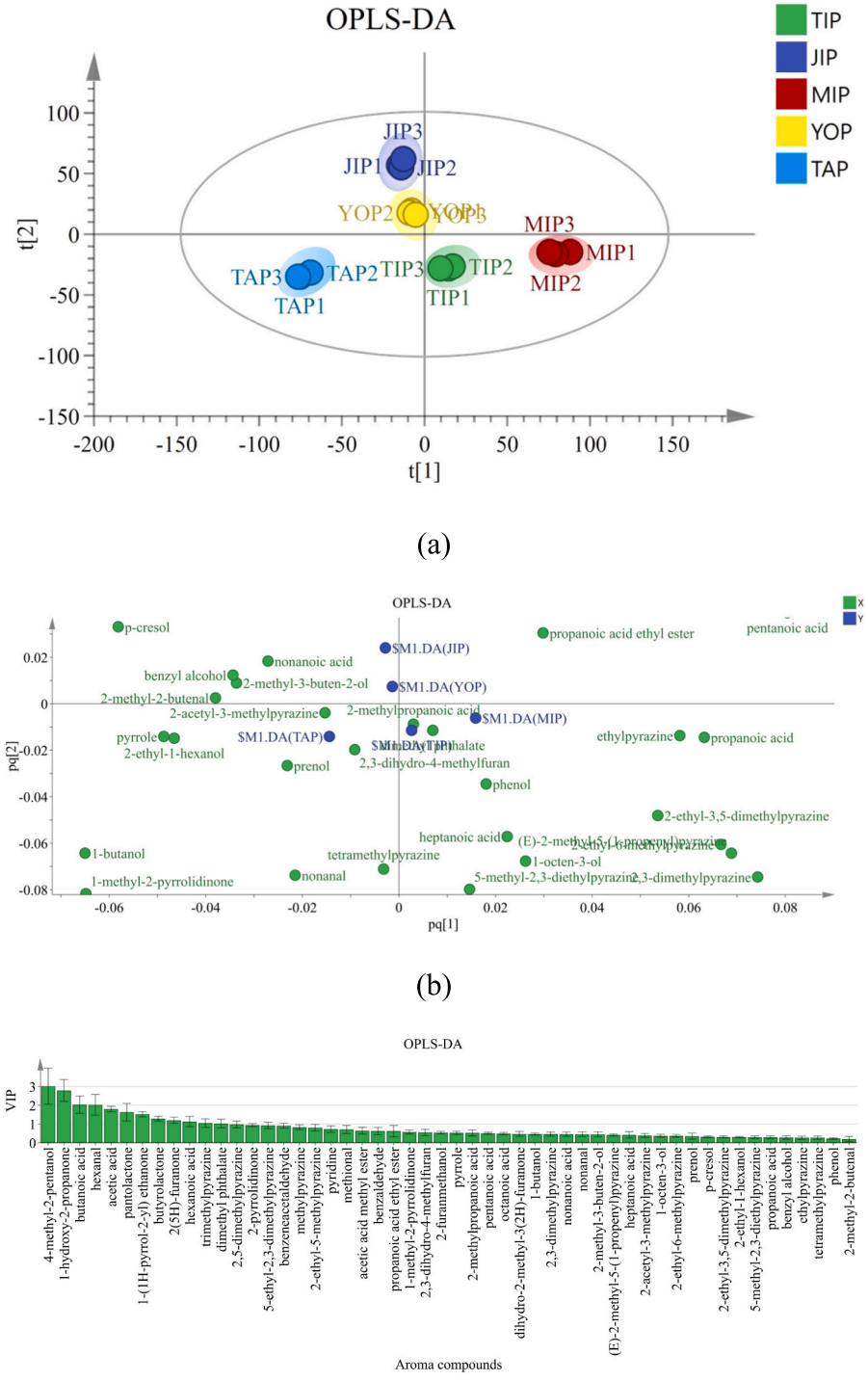

Fig. 3. OPLS-DA of aroma compounds in roasted pork from five species.
(a) Score scatter plot. (b) Loading scatter plot. (c) VIP plot.

concentrations and conformations (Perez Juan, Flores, & Toldra, 2007). The TIP and MIP samples appear to be more suitable for roasting, given their richer aroma profiles and higher concentrations of key aroma compounds, particularly MIP.

3.3. Potential biomarkers analysis for discriminating differential roasted pork

To elucidate the differences among roasted pork from the five species, a supervised OPLS-DA model was established. As shown in Fig. 3a, the model demonstrated excellent stability ($R^2X = 0.99$, $R^2Y = 1$, $Q^2 = 0.99$). Roasted pork samples from the five species were clearly discriminated without any overlap. TIP and MIP samples showed positive scores along component one (t_1), significantly separating them from the roasted pork of the other three species. TAP samples, on the other hand, presented negative scores along component two (t_2), placing them solely in the third quadrant, distinct from the JIP and YOP samples. Notably, only JIP and YOP samples had positive scores along t_2, with no overlap between the two. To identify which aroma compounds were responsible for the observed differences between samples, the

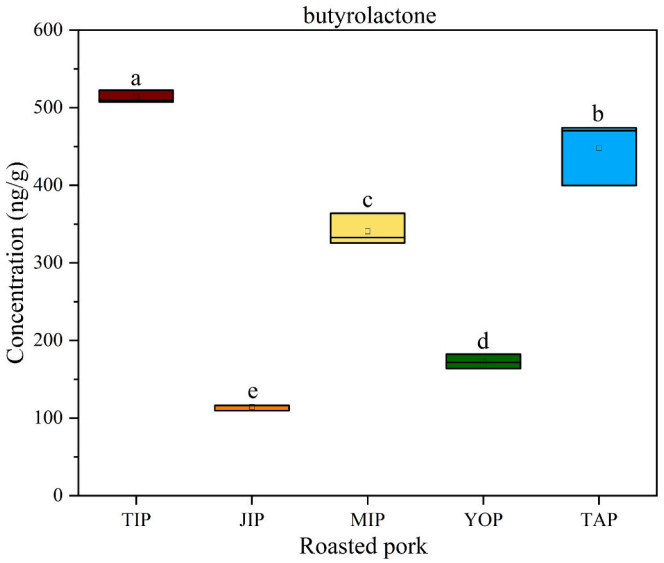

Fig. 4. Box plots of biomarkers in roasted pork from five species.

relationship between the samples and the odorants was established (Fig. 3b). Specifically, 2-methylpropanoic acid, dimethyl phthalate, ethylpyrazine, propanoic acid, heptanoic acid, 2-ethyl-3,5-dimethylpyrazine, 5-methyl-2,3-diethylpyrazine, 2-ethyl-6-methylpyrazine, and 1-octen-3-ol were located in the fourth quadrant, in proximity to the TIP and MIP samples. The compounds containing 2-acetyl-3-methylpyrazine, 2-methylpropanoic acid, pyrrole, 2-ethyl-1-hexanol, prenol, and 2,3-dihydro-4-methylfuran were close to the TAP sample. Additionally, the nonanoic acid, benzyl alcohol, 2-methyl-3-buten-2-ol, and 2-methyl-2-butenal were near the JIP and YOP samples. These findings suggested that TIP, MIP, and TAP samples might exhibit stronger roasty aromas.

As presented in Fig. 3c, twelve odorants were identified with VIP scores greater than 1, including 4-methyl-2-pentanol (3.02), 1-hydroxy-2-propanone (2.79), butanoic acid (2.04), hexanal (2.03), acetic acid (1.80), pantolactone (1.64), 1-(1H-pyrrol-2-yl)ethanone (1.52), butyrolactone (1.29), 2(5H)-furanone (1.20), hexanoic acid (1.13), trimethylpyrazine (1.05), and dimethyl phthalate (1.02). To identify potential aroma biomarkers, the criteria of VIP > 1 and $p < 0.05$ were applied. As shown in Fig. 4, the butyrolactone was identified as a key biomarker for discriminating roasted pork from the five species. The highest butyrolactone concentration was found in TIP samples (513.13 ng/g), followed by TAP (448.01 ng/g) and MIP (340.63 ng/g), while YOP (172.56 ng/g) and JIP (114.02 ng/g) showed lower concentrations. This finding further confirms the utility of OPLS-DA as an effective tool for discriminating different samples (Liu et al., 2024). Interestingly, these results contrast with previous findings, among which 2,3-dimethylpyrazine and trimethylpyrazine are identified as potential biomarkers for distinguishing roasted pork prepared using four thermal methods (Liu, Ma, et al., 2024). In addition, nonanal, dimethyl disulfide, and 2-ethyl-3,5-dimethylpyrazine were important biomarkers for differentiating roasted pork during the air-frying process (Li et al., 2024). The volatile compounds with carbonyl groups, such as hexanal, heptanal, and 3-hydroxy-2-butanone, are identified with VIP scores greater than 1 and are considered potential freshness biomarkers for pork during the storage (Li et al., 2022). These results provide new biomarkers for distinguishing roasted pork from different species, which differ from previous findings related to roasting methods, processes, and storage.

4. Conclusion

The roasted pork from the five species exhibited strong roasty notes, primarily influenced by key aroma compounds such as 5-ethyl-2,3-dimethylpyrazine, 5-methyl-2,3-diethylpyrazine, and 2-acetyl-3-methylpyrazine. The volatilomics combined with OPLS-DA effectively distinguished the aroma profiles of the different species, with butyrolactone identified as a critical biomarker. Among the species, Tibetan pigs (TIP) and Min pigs (MIP) were found to be more suitable for roasting, offering enhanced aroma intensity compared to the other three species. For the food industry, the use of Tibetan and Min pig breeds in roasting could improve the overall aroma profile of pork products. The future study will focus on systematically analyzing the role of proteins and lipids in the formation and retention of aroma compounds in roasted pork, offering deeper insights into the mechanisms driving aroma development.

CRediT authorship contribution statement

Lin Li: Writing – original draft, Resources, Investigation. **Pingping Huang:** Writing – review & editing, Methodology, Formal analysis. **Rujie Yang:** Resources, Investigation, Data curation. **Jingyu Li:** Writing – original draft, Validation, Data curation. **Yuping Zhang:** Validation, Software. **Junke Li:** Writing – review & editing, Formal analysis. **Jianjun Li:** Writing – review & editing, Formal analysis. **Jianmei Zhang:** Resources, Investigation. **Nigel P. Brunton:** Writing – review & editing. **Huan Liu:** Writing – review & editing, Project administration, Methodology, Funding acquisition. **Xiangru Wei:** Writing – review & editing, Supervision, Conceptualization.

Declaration of competing interest

The authors declare that they have no known competing financial interests or personal relationships that could have appeared to influence the work reported in this paper.

Acknowledgements

This study has been financially supported by Ludong University Program (20230044).

Data availability

Data will be made available on request.

References

Dach, A., & Schieberle, P. (2021). Changes in the concentrations of key aroma compounds in oat (*Avena sativa*) flour during manufacturing of oat pastry. *Journal of Agricultural and Food Chemistry, 69*(5), 1589–1597.

Dannenberger, D., Lorenz, S., Nuernberg, G., Scollan, N., Ender, K., & Nuernberg, K. (2006). Analysis of fatty aldehyde composition, including 12-methyltridecanal, in plasmalogens from longissimus muscle of concentrate- and pasture-fed bulls. *Journal of Agricultural and Food Chemistry, 54*(1), 182–188.

Edgar Herkenhoff, M., Brödel, O., & Frohme, M. (2024). Aroma component analysis by HS-SPME/GC–MS to characterize lager, ale, and sour beer styles. *Food Research International, 194*, Article 114763.

Fan, M., Xiao, Q., Xie, J., Cheng, J., Sun, B., Du, W., Wang, Y., & Wang, T. (2018). Aroma compounds in chicken broths of Beijing Youji and commercial broilers. *Journal of Agricultural and Food Chemistry, 66*(39), 10242–10251.

Gąsior, R., Wojtycza, K., Majcher, M. A., Bielińska, H., Odrzywolska, A., Bączkowicz, M., & Migdał, W. (2021). Key aroma compounds in roasted white kołuda goose. *Journal of Agricultural and Food Chemistry, 69*(21), 5986–5996.

Gerlach, C., Leppert, J., Santiuste, A. C., Pfeiffer, A., Boeker, P., & Wust, M. (2018). Comparative aroma extract dilution analysis (cAEDA) of fat from tainted boars, castrated male pigs, and female pigs. *Journal of Agricultural and Food Chemistry, 66*(10), 2403–2409.

Ho, C. T., & Hartman, T. G. (1994). Volatile formation by lipid-mediated Maillard reaction in model systems. In Y. Zhang, et al. (Eds.), *ACS symposium series* (pp. 49–60). Washingtonlipids in food flavors.

Huang, T. C., Bruechert, L. J., Hartman, T. G., Rosen, R. T., & Ho, C. T. (1987). Effect of lipids and carbohydrates on thermal generation of volatiles from commercial zein. *Journal of Agricultural and Food Chemistry, 35*(6), 985–990.

Jo, Y., An, K. A., Arshad, M. S., & Kwona, J. H. (2018). Effects of e-beam irradiation on amino acids, fatty acids, and volatiles of smoked duck meat during storage. *Innovative Food Science and Emerging Technologies, 47*, 101–109.

Li, H., Geng, W., Haruna, S. A., Zhou, C., Wang, Y., Ouyang, Q., & Chen, Q. (2022). Identification of characteristic volatiles and metabolomic pathway during pork

storage using HS-SPME-GC/MS coupled with multivariate analysis. *Food Chemistry, 373*, Article 131431.
Li, J., Zhang, Y., Zhang, R., Yang, R., Ma, Q., Wang, Z., Li, P., Xing, J., Gao, P., Liu, H., & Gong, H. (2024). Unraveling the formation mechanism of aroma compounds in pork during air frying using UHPLC-HRMS and Orbitrap Exploris GC-MS. *Food Research International, 192*, Article 114816.
Liang, B., Li, J., Zhao, S., Pan, X., Zhang, Y., Gao, P., Li, P., Xing, J., Suleman, R., Gong, H., & Liu, H. (2024). Comprehensive analysis of key aroma compounds enhanced by Tamarix ramosissima Ledeb in mutton roasted by air-frying roast technology by means of SAFE-GC-O-MS and lipidomics. *Food Chemistry: X, 23*, Article 101593.
Liu, H., Li, J., Hamid, N., Li, J., Sun, X., Wang, F., Liu, D., Ma, Q., Sun, S., & Gong, H. (2023). Characterization of key aroma compounds in Chinese smoked duck by SAFE-GC-O-MS and aroma-recombination experiments. *Food Chemistry: X, 20*, Article 100997.
Liu, H., Li, J., Zhang, Y., Li, L., Gong, H., Tan, L., Gao, P., Li, P., Xing, J., Liang, B., & Li, J. (2024). Formation and retention of aroma compounds in pigeons roasted by circulating non-fried roast technique by means of UHPLC-HRMS and GC-O-MS. *Food Chemistry, 456*, Article 139960.
Liu, H., Liu, D., Suleman, R., Gao, P., Li, P., Xing, J., Ma, Q., Hamid, N., Wang, P., & Gong, H. (2023). Understanding the role of lipids in aroma formation of circulating non-fried roasted chicken using UHPLC-HRMS-based lipidomics and heat transfer analysis. *Food Research International, 173*, Article 113370.
Liu, H., Ma, Q., Xing, J., Li, P., Gao, P., Hamid, N., Wang, Z., Wang, P., & Gong, H. (2024). Exploring the formation and retention of aroma compounds in ready-to-eat roasted pork from four thermal methods: A lipidomics and heat transfer analysis. *Food Chemistry, 431*, Article 137100.
Majcher, M., & Jeleń, H. H. (2009). Comparison of suitability of SPME, SAFE and SDE methods for isolation of flavor compounds from extruded potato snacks. *Journal of Food Composition and Analysis, 22*(6), 606–612.
Majcher, M. A., Klensporf-Pawlik, D., Dziadas, M., & Jeleń, H. H. (2013). Identification of aroma active compounds of cereal coffee brew and its roasted ingredients. *Journal of Agricultural and Food Chemistry, 61*(11), 2648–2654.
Mu, S., Ni, N., Zhu, Y., Boesveldt, S., & Stieger, M. (2023). How volatile composition facilitates olfactory discrimination of fat content in beef and pork. *Food Research International, 174*, Article 113637.
Murat, C., Gourrat, K., Jerosch, H., & Cayot, N. (2012). Analytical comparison and sensory representativity of SAFE, SPME, and purge and trap extracts of volatile compounds from pea flour. *Food Chemistry, 135*(3), 913–920.
Nie, R., Zhang, C., Liu, H., Wei, X., Gao, R., Shi, H., Zhang, D., & Wang, Z. (2024). Characterization of key aroma compounds in roasted chicken using SPME, SAFE, GC-O, GC–MS, AEDA, OAV, recombination-omission tests, and sensory evaluation. *Food Chemistry: X, 21*, Article 101167.
Niu, Y., Zhang, J., Xiao, Z., & Zhu, J. (2020). Evaluation of the perceptual interactions between higher alcohols and off-odor acids in Laimao baijiu by σ–τ plot and partition coefficient. *Journal of Agricultural and Food Chemistry, 68*(50), 14938–14949.
Perez Juan, M., Flores, M., & Toldra, F. (2007). Binding of aroma compounds by isolated myofibrillar proteins: Effect of protein concentration and conformation. *Food Chemistry, 105*(3), 932–939.
Phetsang, H., Panpipat, W., Undeland, I., Panya, A., Phonsatta, N., & Chaijan, M. (2021). Comparative quality and volatilomic characterisation of unwashed mince, surimi, and pH-shift-processed protein isolates from farm-raised hybrid catfish (Clarias macrocephalus × Clarias gariepinus). *Food Chemistry, 364*, Article 130365.
Schieberle, P. (1995). New developments in methods for analysis of volatile flavor compounds and their precursors. In A. G. Gaonkar (Ed.), *Characterization of food: Emerging methods* (pp. 403–431). Amsterdam: Elsevier.
Selli, S., Gubbuk, H., Kafkas, E., & Gunes, E. (2012). Comparison of aroma compounds in dwarf Cavendish banana (*Musa* spp. AAA) grown from open-field and protected cultivation area. *Scientia Horticulturae, 141*, 76–82.
Shi, H., Gao, R., Liu, H., Wang, Z., Zhang, C., & Zhang, D. (2024). Qualitative and quantitative assessment of key aroma compounds, advanced glycation end products and heterocyclic amines in different varieties of commercially roasted meat products. *Food Chemistry, 436*, Article 137742.
Wang, X., Wang, X., Zhang, X., Liu, S., Yu, J., Cui, H., … Ho, C. T. (2023). Changes of lipid oxidation, volatile and taste-active compounds during pan-heating of pork belly. *Food Research International, 172*, Article 113106.
Xie, J., Sun, B., Zheng, F., & Wang, S. (2008). Volatile flavor constituents in roasted pork of Mini-pig. *Food Chemistry, 109*(3), 506–514.
Yan, X., Yang, M., He, Q., Sun, S., Zhang, Y., Feng, X., He, M., Liu, T., Li, Y., & Zhang, F. (2021). An integrated method for monitoring thermal processing temperature of pork based on Q-Exactive mass spectrometry and chemometrics. *Journal of Chromatography A, 1644*, Article 462083.
Yang, X., Pei, Z., Du, W., & Xie, J. (2023). Characterization of volatile flavor compounds in dry-rendered beef fat by different solvent-assisted flavor evaporation (SAFE) combined with GC-MS, GC-O, and OAV. *Foods, 12*(17), 3162.
Yao, Y., Huang, M., Wang, X., Yu, J., Cui, H., Hayat, K., … Ho, C. T. (2024). Characteristic volatile compounds contributed to aroma of braised pork and their precursor sources. *Food Chemistry, 459*, Article 140335.
Yu, T. S., & Ho, C. T. (1995). Volatile compounds generated from thermal reaction of methionine and methionine sulfoxide with or without glucose. *Journal of Agricultural and Food Chemistry, 43*(6), 1641–1646.
Zhang, R., Zhang, Y., Sun, Y., Yu, H., Yang, F., Guo, Y., Xie, Y., & Yao, W. (2022). High-intensity ultrasound promoted the aldol-type condensation as an alternative mean of synthesizing pyrazines in a Maillard reaction model system of D-glucose-$^{13}C_6$ and L-glycine. *Ultrasonics Sonochemistry, 82*, Article 105913.
Zhao, L., Erasmus, S., Yang, P., Huang, F., Zhang, C., & van Ruth, S. (2023). Establishing the relations of characteristic aroma precursors and volatile compounds for authenticating Tibetan pork. *Food Chemistry, 427*, Article 136717.
Zhu, Y., Dong, J., Jin, J., Liu, J., Zheng, X., Lu, J., Liang, Y., & Ye, J. (2021). Roasting process shaping the chemical profile of roasted green tea and the association with aroma features. *Food Chemistry, 353*, Article 129428.